Uncertainty of protein-ligand binding constants: asymmetric confidence intervals *versus* standard errors

Vaida Paketurytė[a], Vytautas Petrauskas[a], Asta Zubrienė[a], Olga Abian[b,c], Margarida Bastos[d], Wen-Yih Chen[e], Maria João Moreno[f], Georg Krainer[g], Vaida Linkuvienė[a], Arthur Sedivy[h], Adrian Velazquez-Campoy[b,i], Mark A. Williams[j] and Daumantas Matulis[a]

[a] Department of Biothermodynamics and Drug Design, Institute of Biotechnology, Life Sciences Center, Vilnius University, Vilnius, Lithuania
[b] Institute of Biocomputation and Physics of Complex Systems (BIFI), Joint Units IQFR-CSIC-BIFI, and GBsC-CSIC-BIFI, Universidad de Zaragoza, Zaragoza, Spain; Aragon Institute for Health Research (IIS Aragon), Zaragoza, Spain; Department of Biochemistry and Molecular and Cell Biology, Universidad de Zaragoza, Zaragoza, Spain; Centro de Investigación Biomédica en Red en el Área Temática de Enfermedades Hepáticas y Digestivas (CIBERehd), Barcelona, Spain
[c] Instituto Aragonés de Ciencias de la Salud (IACS), Zaragoza, Spain
[d] CIQ-UP, Department of Chemistry and Biochemistry, Faculty of sciences, University of Porto, Portugal
[e] Department of Chemical and Materials Engineering, National Central University, Taoyuan, Taiwan
[f] Coimbra Chemistry Center, Chemistry Department, Faculty of Sciences and Technology, University of Coimbra, 3004-535 Coimbra, Portugal
[g] Yusuf Hamied Department of Chemistry, University of Cambridge, Cambridge, United Kingdom
[h] Protein Technologies, Vienna Biocenter Core Facilities GmbH, Vienna, Austria
[i] Fundacion ARAID, Government of Aragon, Zaragoza, Spain
[j] Institute for Structural and Molecular Biology, Department of Biological Sciences, Birkbeck, University of London, United Kingdom

Corresponding authors (of the WG4 of a COST network project CA15126**):**
Daumantas Matulis
Address: Saulėtekio 7, Vilnius LT-10257, Lithuania
Tel. +370-5-223-4364
Fax. +370-5-223-4367
Email: daumantas.matulis@bti.vu.lt, matulis@ibt.lt
Margarida Bastos: mbastos@fc.up.pt
Arthur Sedivy: arthur.sedivy@vbcf.ac.at
AdrianVelazquez-Campoy: adrianvc@unizar.es
Mark A. Williams: ma.williams@bbk.ac.uk

Abstract

Equilibrium binding constants (K_b) between chemical compounds and target proteins or between interacting proteins provide a quantitative understanding of biological interaction mechanisms. Reporting uncertainties of measured experimental parameters are critical for decision making in many scientific areas, e.g., in lead compound discovery processes and in comparing computational predictions with experimental results. Uncertainties in measured K_b values are commonly represented by a symmetric normal distribution, often quoted in terms of the experimental value plus-minus the standard deviation. However, in general the distributions of measured K_b (and equivalent K_d) values and the corresponding free energy change ΔG_b are all asymmetric to varying

degree. Here, using a simulation approach, we illustrate the effect of asymmetric K_b distributions within the realm of isothermal titration calorimetry (ITC) experiments. Further we illustrate the known, but perhaps not widely appreciated, fact that when distributions of any of K_b, K_d and ΔG_b are transformed into each other their degree of asymmetry is changed. Consequently, we recommend that a more accurate way of expressing the uncertainties of K_b, K_d, and ΔG_b values is to consistently report 95% confidence intervals, in line with other author's suggestions. The ways to obtain such error ranges are discussed in detail and exemplified for a binding reaction obtained by ITC.

Keywords
Isothermal titration calorimetry; confidence intervals; standard error; log-normal distribution; dissociation constant; binding constant.

Introduction

Interactions between biomolecules are central to many areas of biomedicine. Protein–protein interactions[1,2] are important, *e.g.,* in immunological antibody–antigen binding reactions[3], or gene regulatory protein – nucleic acid interactions[4–6]. Furthermore, interactions of small molecular weight compound with proteins are fundamental to the action of many metabolic enzymes, and their regulators and in drug discovery during the search for lead compounds, as well as in the final characterization of promising therapeutic drugs[7–9].

Numerous techniques are used to determine biomolecular interactions[8,10], such as the inhibition of enzymatic activity[11], surface plasmon resonance[12–14], isothermal titration calorimetry (ITC)[15–20], thermal shift assay (differential scanning fluorimetry)[21–25] and numerous others[8]. All these techniques are expected to provide comparable values of intermolecular interaction affinities provided that measurements are feasible at nearly identical conditions.

Reporting the errors of association reactions must be done consistently and accurately in order to enable reliable interpretation and reuse of results[26]. In most scientific literature the uncertainty (i.e., the repeatability) of a binding equilibrium measurement is expressed as ±x (or x%, accounting for the standard deviation or error) of the measured value, with the underlying assumption that the measured affinity values are distributed randomly according to a normal (i.e., Gaussian) statistical distribution[15,27–40]. For a normal distribution, the reported ±x-value typically corresponds to the 68.3% symmetric confidence interval ($CIs_{,68.3}$). In some cases, the reported symmetric uncertainty is estimated from analysis of several repeated measurements via the appropriate Student's *t*-distribution. However, the uncertainty is frequently retrieved only from the fitting program used to estimate the parameter from a single set of experimental data[41]

The equilibrium binding constant K_b (also referred to as the association or affinity constant) is inversely related to the dissociation equilibrium constant $K_d = 1/K_b$ and is related to the change in the standard Gibbs energy upon binding, ΔG_b, (often written with the naught symbol, ΔG_b^o, which is omitted here for terms of simplicity) by the equations: $\Delta G_b = -RT \ln K_b$, or $K_b = e^{-\Delta G_b / RT}$. These logarithmic, exponential, and reciprocal relationships do not preserve the shape of distribution of values. For example, a continuous probability distribution of a random variable, whose logarithm is normally distributed follows a log-normal distribution, taking only positive, real values. Therefore, if a normal distribution is assumed for ΔG_b, K_b must have a log-normal distribution.

The inherent asymmetry in parameter distribution has consequences for the reporting of errors. Symmetric ±x-value are not an appropriate way of accurately expressing the uncertainty for ΔG_b, K_b and related values. Asymmetric *F*-statistics-associated CIs have been introduced as an elegant approach to report error ranges and the propagation of CIs in nonlinear, asymmetrical variance spaces, accounting for non-normal distributed parameter distributions, including ΔG_b, K_b and K_d[42–46].

In this work we explore in detail the unrealistic nature of the assumption of a normal distribution of K_b, K_d and other thermodynamic quantities through various examples and evaluate a practical approach, based on previously established procedures[42–45], to obtain estimates of the asymmetric *F*-statistics-associated CIs that are both simpler to treat consistently in transforming between different expressions for the affinity and better reflect the real uncertainties in the data.

Results and discussion

We use simulated distribution curves to show how the mathematical relationships between the parameters K_b, K_d, and ΔG_b affect the asymmetry of their distributions.

Case 1. Transformation of the distribution of K_b and ΔG_b values assuming that each has a normal distribution

Here we show how transformations of K_b and ΔG_b values results in an asymmetry of their distributions. For this, we assumed that either K_b or ΔG_b values are normally distributed and generated a set of 10000 random K_b's with mean value 2×10^7 M^{-1} and standard deviation of $\pm 0.6 \times 10^7$ M^{-1} (Figure 1A) and a set of 10000 random ΔG_b's with mean value –41.67 kJ/mol and standard deviation of ±0.77 kJ/mol (Figure 1D). Note that $K_b = 2 \times 10^7$ M^{-1} corresponds to ΔG_b = –41.67 kJ/mol at 25 ºC. Each set of values is then converted to the other representation through the appropriate logarithmic or exponential formula (Figure 1 B and E), and in both cases to the dissociation constant K_d (Figure 1 C and F). These transformations show that the Gibbs energy change, and the binding and dissociation constants do not follow a normal distribution at the same time. The transformation between K_b and ΔG_b in either direction introduces a similar amount of skew into the distribution, and that the transformation between K_b and K_d may impart even greater skew.

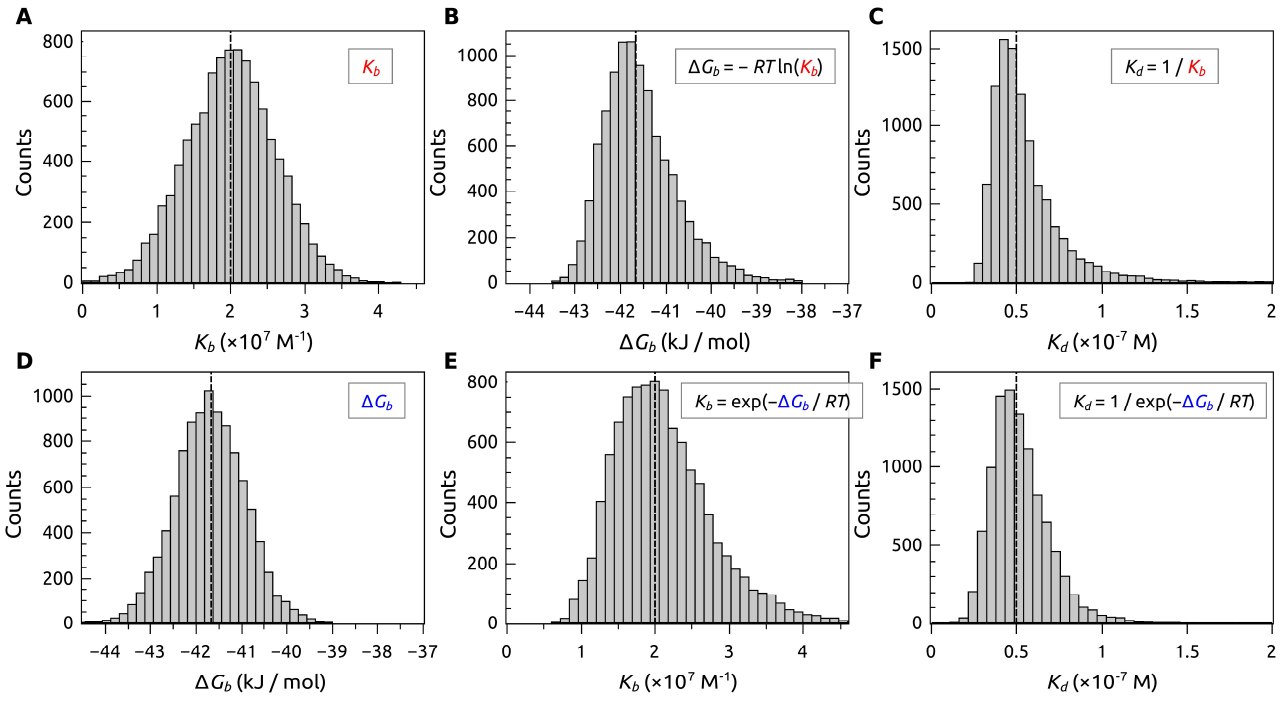

Figure 1. Illustrating the effect of transformation of K_b and ΔG_b values into each other and into K_d distributions of protein-ligand binding. (A) Distribution of 10000 random values of K_b generated for a normal distribution with mean 2 × 10^7 M^{-1} and standard deviation of ±0.6 × 10^7 M^{-1}. (B) Distribution of ΔG_b values calculated from the 10000 K_b values in (A). (C) The distribution of dissociation constants K_d corresponding to data in (A). (D) Distribution of 10000 random values of the Gibbs energy of binding generated for a normal distribution with mean –41.67 kJ/mol and a standard deviation of 0.77 kJ/mol. (E) Distribution of K_b values calculated from the ΔG_b values in (D). (F) The dissociation constant calculated from (D). The logarithmic transformation introduces a skew of 1.3 (B) and the exponential transformation a skew of 0.9 (E) from the normal distributions. The greatest skewness arises from the transformation of the normally distributed K_b to K_d (skew is equal to 4.3 in (C)).

When considering the kinetics of the interactions, inaccuracies in the reported parameters (most probable value and uncertainty) may be even more severe. The rate constants are related with the Gibbs energy variation between the reactants and the transition state through an exponential function, and this energy variation is usually larger than that observed between the reactants and the products of the transformation. This situation is analyzed in the Supplementary Material.

Confidence intervals are a consistent and inter-convertible way to accurately represent measurement uncertainty

The previous illustration shows that it is not warranted to use a symmetric ±x-value as an accurate expression of the uncertainty for all three quantities ΔG_b, K_b and K_d describing the same physical equilibrium. For consistent reporting of uncertainties in experimental data it is always necessary to state the range of uncertainty [x_{low}, x_{high}] which makes apparent any degree of asymmetry. Asymmetry in any skewed distribution is more evident toward its extremes, thus the use of a central 68.3% confidence interval does not effectively describe the asymmetry. Consequently, it is advantageous for clear description to report the larger 95% confidence interval (CI_{95}), which in any

case typically better represents the range in which the true value of the parameter is likely to be found.

Given that a normally distributed ΔG_b is transformed into a log-normal distribution for K_b, one could imagine that given some CI for ΔG (symmetrical) it might be required to calculate the 95% confidence interval of this log-normal distribution to obtain uncertainties in K_b. However, as the individual values for the quantities are correctly transformed by the exponential, logarithmic and reciprocal relationships, it is simple to directly convert the lower and upper values of any confidence interval between representations (this is rigorously true for one-to-one mono-parametric conversions). For example, using the $\Delta G_b = -41.67 \pm 0.77$ kJ/mol from Case 1 gives a CI_{95} = [-43.18, -40.16] for ΔG_b (as 95% CI limits are $1.96 \times \sigma$ for a normal distribution in the limit of a large number of data points). The upper limit of the CI interval for $K_b = \exp(-\Delta G_{b,lower}/RT) = \exp(43.18/2.47896) = 3.68 \times 10^7$ M^{-1}. Similar transformation for the lower limit gives a CI_{95} = $[1.09, 3.68] \times 10^7$ M^{-1} (which can be seen to match with the distribution in Figure 1E for which the CI_{95} is $[1.09, 3.69] \times 10^7$ M^{-1}). Thus, consistently reporting CI_{95} makes it easy to transform between representations preserving all information regarding uncertainties in experimental values. This procedure also eliminates the possibility of getting error intervals with negative values for the equilibrium constants.

The logarithmic relationship between K_b and ΔG_b, is also important for other practical purposes such as calculating averages from a set of determinations. The mean of several ΔG_b values can be calculated using the arithmetic average, while the mean of several K_b values should be calculated using the geometric average. Alternatively, the value to report for K_b can be calculated from the obtained arithmetic average of ΔG_b values. That way, the correspondence between ΔG_b and K_b averages is maintained in the same way that the correspondence between confidence interval limits is maintained.

Case 2. Simulated error distributions for ITC measurements of 1:1 binding

The preceding hypothetical illustrations (Case 1) leave open the question of whether the uncertainty in any parameter might be expected to have a strongly asymmetric or near normal distribution, and, if so, under what circumstances. To investigate these issues, we simulated the impact of binding affinity changes on the variability of ITC experiments.

In common with many methods for obtaining binding constants, ITC experiments are performed as a titration where successive injections of one reactant species into a fixed amount (or concentration) of the other species leads to progressive saturation of a binding site. A signal monitors formation of the bound form and the values for the signal (transformed into heat, Q) are fit to an equation describing the relationship between the heat released or absorbed and the thermodynamic parameters K_b (or ΔG_b), the enthalpy change ΔH_b and the apparent stoichiometry, that are thus determined as parameters of the fit. The measurement errors are typically propagated to the fitted parameters in a way that depends on the equation describing the titration and a range of experimental variables, e.g., the number of injections, the final degree of saturation and concentrations of reactants.

The measurement's variability for the heat of each injection is random normally distributed (as it

arises from the combined random effects of mechanical variability of the injection volume, electrical noise and how these impact upon the software process for integrating the heat signal for each injection).

To simulate the effect of measurement variation, random values from an appropriate normal distribution are added to the theoretically expected injection heat values for an ideal 1:1 binding reaction. The simulations used here model a VP-ITC instrument (MicroCal/Malvern). Tellinghuisen has determined that for this instrument (when set for high maximum injection heats) the standard deviation of measurements (when including the effect of subtracting blanks or heats of dilution) is approximately constant at 3 μJ for injections of heat < 500 μJ[47]. Recently alternative error models with a smaller constant standard deviation of 0.5-0.9 μJ plus an injection-heat dependent term of 0.002-0.01uJ per uJ (not including effects of subtraction) have been proposed[48,49] . We use the original injection-heat independent error model here, but note that it may overestimate the error for an optimally set up instrument for a low-heat biochemical reaction, however the absolute value of the error is not critical as it is the proportional error (the signal to noise) that influences the shape of the parameter error distribution. The variation of the fitted parameters, K_b (and the corresponding ΔG_b) and ΔH_b across 10000 Monte Carlo simulated 1:1 binding reactions of fixed stoichiometry are shown in Figure 2. The simulations performed here calculate the dilution effects on reactant concentrations occurring during the titration and modification of injection heats due to the volume displaced from the reaction cell following a discrete inject step model (or instantaneous injection model) [50]. The simulated experiments are then fitted using an unweighted least-squares fit to the Wiseman equation[51] following typical experimental data analysis practice.

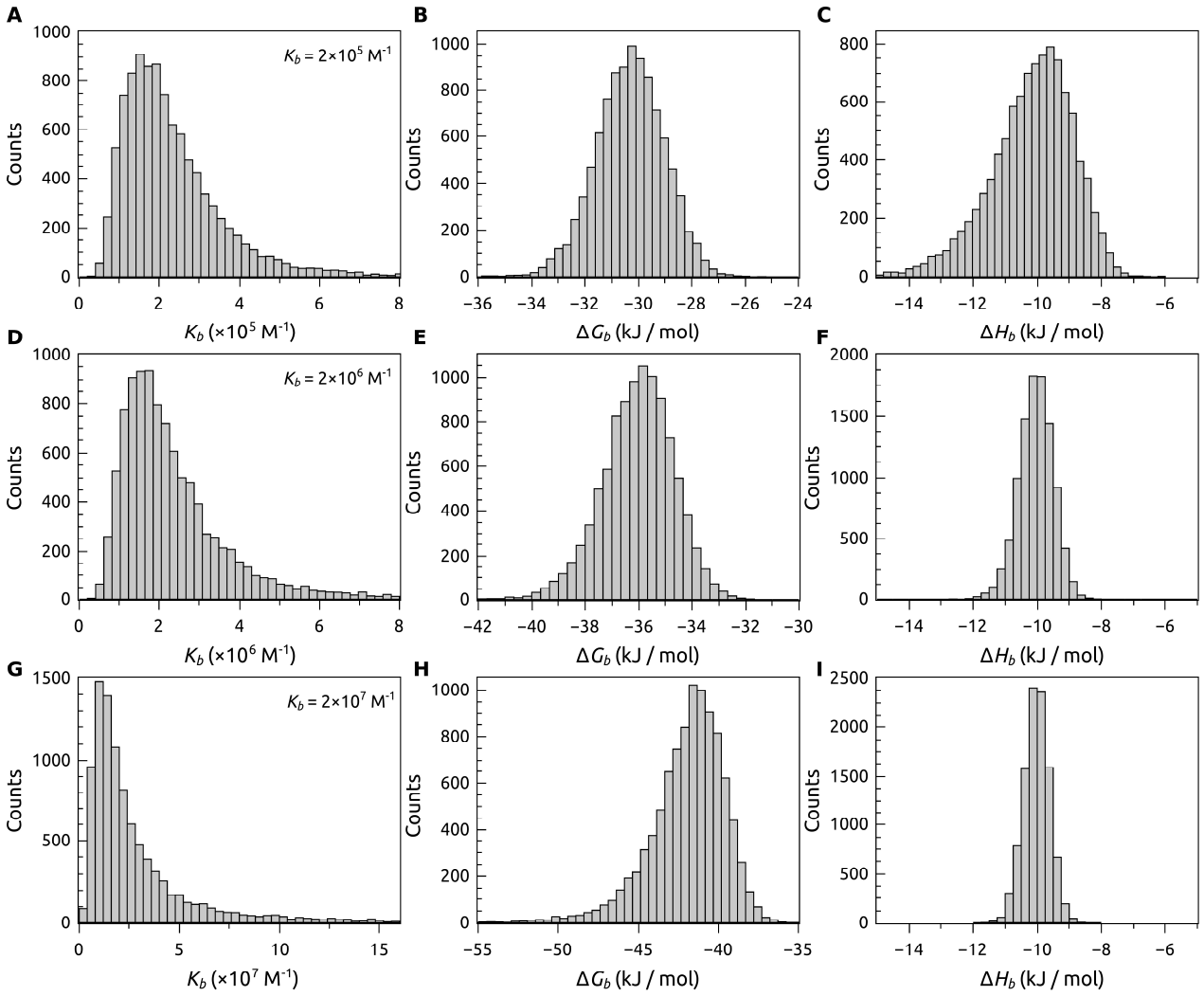

Figure 2. Monte Carlo simulation modelling of variation in the fitted parameters of ITC experiments for three different binding affinities – (A-C) 2 × 10^5 M^{-1}, (D-F) 2 × 10^6 M^{-1} and (G-I) 2 × 10^7 M^{-1}. For each binding affinity, 10,000 simulated data sets were created. All simulations were for a 1:1 binding reaction with molar enthalpy change ΔH_b = -10 kJ/mol, 20×15 µL injections of 200 µM ligand into 20 µM protein leading to a final ligand:protein ratio of 2.5:1. The simulations are modelling a VP-ITC instrument and a measurement error of standard deviation of 3 µJ per injection. Datasets not achieving a satisfactory fit are excluded.

The simulations show that for all three true K_b values the expected variation in the observed value is asymmetrically distributed. Furthermore, increasing the magnitude of K_b increases both the range of variation and the positive skew of the distribution of the K_b values (Table 1), *i.e.* there is an increasing tendency to observe more frequently higher than lower affinity values as K_b increases, thus the higher K_b values become more likely to occur. For this particular experimental scenario, we find that there is an 8% probability of observing a K_b less than half, and a 9% chance of more than twice the true value when K_b = 2×10^5 M^{-1}. Those probabilities respectively increase to 18% and 24% when the assumed K_b = 2×10^7 M^{-1} (and the probability of an observation more than 4× the true value is 12%).

The simulated scenario in Figure 2 has relatively low injection heats of approximately 1/3rd of the average for protein ligand interactions in a recent large-scale study[52] and with high proportional measurement errors. These values have been chosen to clearly illustrate the various effects on the

distributions of increasing affinity. Since the asymmetry increases with proportional measurement error[49], observed asymmetries would be smaller for most experimental cases where those errors are smaller. Even in this simulated experimental scenario the resulting ΔG_b distribution has little asymmetry except at the highest affinity and conversely the enthalpy change is only appreciably asymmetric and has greater uncertainty at the lowest affinity. In particular, we note that in this experimental scenario even with its quite large proportional measurement ΔG_b is near normally distributed for reasonably optimal experiments (Wiseman parameters C of 4 and 40 respectively for the first two simulations).for less optimal experiments (Wiseman parameter of 400 for the last simulation) skewness can be readily seen. This can most likely be attributed to the fact that for a 20-point ITC experiment with the parameters used for the simulation essentially only 3-4 datapoints fall into the transition region and any noisy data here will have a bigger influence to larger deviations (long tailing to higher K_b values). Also seen is an inverse relationship between the variations in measured affinity and enthalpy, this is expected due to the shape of the titration curve changes appreciably with binding affinity under the experimental conditions we have simulated with fixed concentration. At high C almost all the ligand binds in the early injections of a titration giving several injection heats with high signal to noise and thus lowering the observed variation in the enthalpy measurement. An inverse relationship between the uncertainties in affinity and enthalpy is generally expected for ITC data. Under the experimental conditions we have simulated with fixed concentrations the shape of the titration curve changes appreciably with binding affinity.

Table 1. Statistical parameters for simulated ITC data at three different binding affinities. Data correspond to the distributions in Figure 2. The 95% confidence intervals CI_{95} are determined directly from central 95% of values of the distributions.

Starting K_b (M^{-1})	**K_b Skew**	**K_b (M^{-1}) CI_{95}**	**ΔG_b (kJ/mol)**	**ΔG_b Skew**	**ΔG_b (kJ/mol) CI_{95}**	**ΔH_b Skew**	**ΔH_b (kJ/mol) CI_{95}**
2×10^5	1.3	[0.78, 5.8] $\times10^5$	-30.26	-0.2	[-32.9, -27.9]	-0.7	[-13.2, -8.0]
2×10^6	1.5	[0.78, 6.5] $\times10^6$	-35.97	-0.4	[-38.9, -33.6]	-0.2	[-11.1, -9.1]
2×10^7	23	[0.51, 22] $\times10^7$	-41.67	-1.1	[-46.7, -38.3]	-0.1	[-10.8, -9.3]

Error estimations for ΔG_b and K_b using asymmetric profile likelihood Confidence Intervals.

Because the calculation is built into most analysis software, most researchers[6-20] report the precision of the affinities between molecules using asymptotic-symmetric confidence intervals ($CI_{S,\alpha}$) calculated using the standard deviation for each parameter, as estimated from the sum of squared residuals, *RSS*, and the covariance matrix from the fitting analysis, and a chosen confidence level α (typically 68.3%) of a t-Student distribution. The experimental and simulated results have shown that this symmetric approach does not communicate and accurately preserve information about uncertainty, and that use of asymmetric F-statistics-associated (or profile likelihood) CI_{95} is both simple and preferable. How then can we estimate CI_{95} in practice, e.g., from single experiments? We will analyze this case here in detail, as it is the simplest one, and for several experiments the reasoning will be basically the same - we suggest to perform a global fit with all individual datasets and get the global confidence intervals.

A possible approach is to fit for ΔG_b and use the capabilities of different software to obtain the asymptotic-symmetric error $CI_{S,95}$ for the Gibbs energy change. Asymmetric confidence intervals for K_b or K_d can then be obtained by simply transformation of the upper and lower limits of the ΔG_b confidence interval. As we have seen that for titration data ΔG_b is less affected by asymmetry, consequently this approach will be effective in many circumstances and is certainly better than current practice. However, it also fails in some circumstances, e.g., for high affinity interactions as shown in Case 2 or where measurement errors are large (as extensively studied previously[49]) so prior knowledge of the theoretically expected behavior of ΔG_b uncertainty for the experiment scenario is required to apply it. Consequently, this approach cannot be generally recommended.

A second possible approach that is applicable in all circumstances is to use a 'bootstrap' procedure in which values of the residuals of the best fit are randomly selected and added to the fitted value at each titration point and the new set of data points so created refitted. Repeating this re-sampling procedure many times (>1000) yields a distribution of values for each fitted parameter from which the confidence intervals can be obtained. This approach is applicable where the measurement variability is constant throughout the titration and produces $CI_{S,95}$ ranges that are only slightly larger than the true values. Unfortunately, the requisite re-sampling procedure is not widely available in commercial software.

We believe that the most practicable way to express the repeatability for K_b and ΔG_b is through calculation of the profile likelihood confidence intervals $CI_{P,\alpha}$ (at statistical significance level α)[42–46], which can be determined by an extension of the typical fitting approach. Once the non-linear least squares regression analysis of N experimental points has been performed with a model with P parameters, the best estimates for the P parameters are obtained with an associated residual sum of squares RSS_0. Ideally, the P parameters could be systematically varied to get a P-dimensional contour fulfilling the expression:

$$RSS = RSS_0\left(1 + \frac{P}{N-P}F_{P,N-P}(\alpha)\right)$$

where $F_{n,m}$ is the Fisher-Snedecor distribution with $n = P$ and $m = N - P$ degrees of freedom, and the α is the chosen confidence level[53]. Within that P-dimensional contour, the different possible sets of P parameters provide RSS values that are not statistically different (at a confidence level α) from RSS_0. Then, by projecting the P-dimensional contour onto the different P axes, the confidence interval for each parameter can be determined. However, this procedure is not practical if there are more than two fitting parameters. Therefore, very often marginal confidence intervals are determined by varying just one parameter at a time[42,54]. Thus, a given parameter, p, is selected and kept fixed at different values, while the RSS is minimized over the remaining free parameters, constructing an RSS (p) curve (RSS as a function of p) is constructed with the resulting minimized RSS values (see Figure 3, right). The two limiting values for the given parameter p defining its profile confidence interval $CI_{P,\alpha}$ will fulfill the expression:

$$RSS(p) = RSS_0\left(1 + \frac{1}{N-P}F_{1,N-P}(\alpha)\right)$$

These two limiting values define the interval in which the parameter p provides RSS values that are

not statistically different (at a confidence level α) from RSS_0. The process can be repeated for each of the other parameters, and all P marginal confidence intervals estimated.

In general, *RSS* is not a symmetric function of the studied parameter with respect to the minimum value RSS_0, and the two limiting values satisfying the previous equation define an asymmetric confidence interval for each parameter. The asymmetry degree and the size of the confidence interval depends on the nature of the parameter considered and the sensitivity of *RSS* to that parameter.

The procedure is illustrated by analyzing an isothermal calorimetric titration simulated (with K_b = 2×10^6 M^{-1}, ΔH = 41.8 kJ/mol, and n = 1) with a chosen noise level (Figure 3) and shown in detail for the Origin software as an example in Supplementary Material (2. Quick calculation of profile likelihood asymmetric confidence intervals $CI_{P,95}$.).

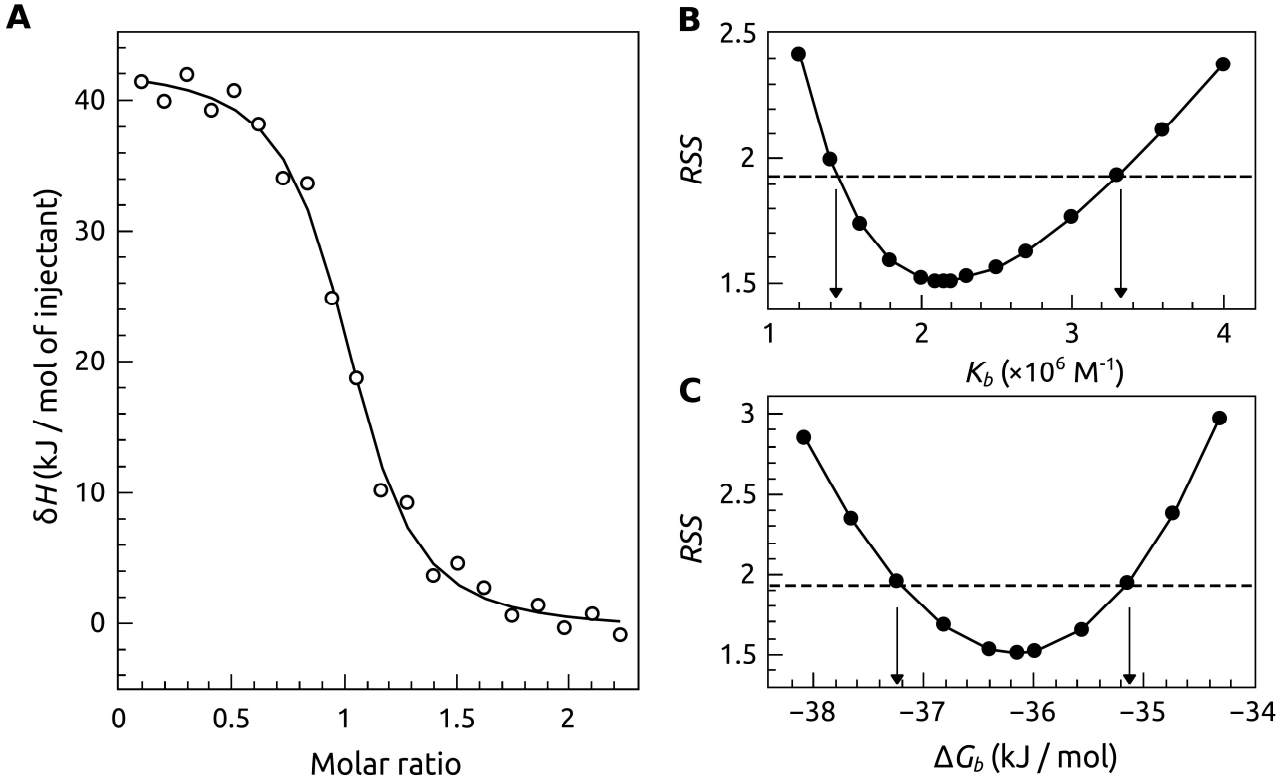

Figure 3. (A) A simulated ITC titration curve corresponding to the $K_b = 2\times10^6$ M^{-1}, ΔH = 41.8 kJ/mol, and 1:1 binding stoichiometry with random measurement error for each injection. The continuous line corresponds to the best fit considering either K_b or ΔG_b as fitting parameters. (B) *RSS* dependence on K_b. (C) *RSS* dependence on ΔG_b. Either K_b or ΔG_b are varied systematically (stepped through fixed values below and above their best estimate) and the remaining parameters are freely adjusted to re-minimize the *RSS*; then, that minimum *RSS* is plotted as a function of either K_b or ΔG_b. The minimum in *RSS* (i.e. RSS_0) corresponds to the best fit (all parameters freely varying, including K_b or ΔG_b). The horizontal dotted line is the limit reference value for *RSS* with 95% confidence, equal to RSS_0 $(1+(1/(N\text{-}P)F_{1,N\text{-}P(0.95)}))$. The intercepts between the *RSS* curve and the reference *RSS* value (indicated by arrows) provide the limits for the confidence intervals. The way to get these CIs with the Origin software is shown in Supplementary Material as an example (2. Quick calculation of profile likelihood asymmetric confidence intervals $CI_{P,95}$.)

The standard output for the best fit to the titration in Figure 3 has the following estimated

parameters: K_b = (2.2 ± 0.4) × 10^6 M^{-1}, ΔH = 43.3 ± 1.2 kJ/mol, and n = 0.99 ± 0.01. If the Gibbs energy of interaction is considered as a fitting parameter instead of K_b the best fit provides the following estimated parameters: ΔG = -36.2 ± 0.4 kJ/mol, ΔH = 43.3 ± 1.3 kJ/mol, and n = 0.99 ± 0.01.

These uncertainties correspond to the typical standard errors $CI_{S,68.3}$ for the fitting parameters generated from the covariance matrix. The asymptotic-symmetric confidence intervals for a confidence level of α = 95% $CI_{S,95}$ are calculated as a multiple of these values determined by the t-Student distribution. The asymptotic-symmetric and asymmetric profile likelihood 95% confidence intervals are shown in Table 2.

Table 2. Best fit parameters and uncertainties determined as asymptotic-symmetric $CI_{S,95}$ and profile likelihood $CI_{P,95}$ confidence intervals

[a] fitting of K_b and calculation of its $CI_{P,95}$ with subsequent transformation to ΔG_b values

[b] fitting of ΔG_b and subsequent calculation of K_b

	K_b (2.2)[a] (× 10^6 M^{-1})	ΔG_b (-36.2) [b] (kJ/mol)	ΔH_b (kJ/mol)	N
$CI_{S,95}$[a]	**[1.29, 3.03]**	[-37.0, -34.9]	[40.8, 45.9]	[0.96, 1.02]
$CI_{S,95}$[b]	[1.44, 3.30]	**[-37.2, -35.1]**	[40.7, 46.0]	[0.96, 1.02]
$CI_{P,95}$[a]	**[1.44, 3.30]**	[-37.2, -35.1]	[40.9, 46.1]	[0.96, 1.03]
$CI_{P,95}$[b]	[1.44, 3.30]	**[-37.2, -35.1]**	[40.9, 46.1]	[0.96, 1.03]

As expected from the previous results, the uncertainty in K_b is revealed to be asymmetric by the profile likelihood confidence interval $CI_{P,95}$. Also as expected from the Monte Carlo simulations (in Case 2) at this binding affinity, the $CI_{P,95}$ for ΔG_b is almost symmetric. Indeed, as discussed above in this case of an actual symmetric uncertainty in ΔG_b, both the asymptotic-symmetric and profile likelihood methods give the same confidence intervals for both parameters provided that ΔG_b is fitted and then transformed to K_b. However, only the profile likelihood approach produces the same results if K_b is fitted. When using $CI_{P,95}$, there is a perfect correspondence between estimated values and uncertainty interval limits for K_b and ΔG_b; thus, no matter which parameter is employed as a fitting parameter, the other parameter and its confidence interval can be readily calculated through their mathematical relationship. However, when using $CI_{S,95}$, the estimated values for K_b and ΔG_b are in correspondence, but the uncertainty intervals are not. The profile likelihood approach is more robust in estimating uncertainties and, thus, the recommended approach.

Conclusions

Although the inherent asymmetry that appears as a result of the measurement error propagating through the data analysis process has been illustrated here with only ITC simulations, they are true

for all binding experiments (i.e., to an extent that depends on the nature of the measurement errors and the equations used to analyze each particular method). The presented concepts and procedures for dealing with this asymmetry to determine accurate uncertainties can be extended to any experimental technique used to determine binding affinities or any related quantities (see the distribution of the kinetic rate constant in the supplementary material). The calculation of the confidence intervals can be performed manually following the step-by-step procedure explained above. These can be conveniently carried out in Excel[42], but fortunately, commercially available software packages (e.g., Origin, GraphPad, Sedphat) also provide profile likelihood confidence intervals, for all fitting parameters at any confidence level, in a user friendly manner, without the need for complicated calculations. Once the best fit is achieved (with all parameters freely varying), the profile likelihood confidence intervals (at a certain confidence level) for all fitting parameters are readily calculated within just a single step as explained in the Supplementary materials.

Considering the variations in the shape and inherent difference of the uncertainty distribution the two thermodynamically related parameters K_b and ΔG_b, reporting a symmetric error appears not to be the scientifically correct way. Reporting 95% confidence intervals removes the artificial restriction of symmetry and enables more accurate reporting of uncertainty. The statistically sound construction of the profile likelihood confidence intervals, and the perfect agreement shown of CIs obtained when the fitting of ITC data was performed for K_b or ΔG_b and ΔH_b, shows that profile likelihood confidence intervals can be used to report the repeatability of K_b and ΔH_b as retrieved from ITC, or for binding affinities determined by any other method.

Acknowledgements

This research was funded by grant no. S-LLT-20-2 from the Research Council of Lithuania (DM). MB and MJM aknowledge Fundação para a Ciência e Tecnologia (FCT), Portugal, for the financial support to Projects UIDB/00081/2020 and UIDB/00313/2020, respectively. The authors also acknowledge the COST action ARBRE-MOBIEU CA15126 supported by COST (European Cooperation in Science and Technology).

References

1. Typas, A. & Sourjik, V. Bacterial protein networks: properties and functions. *Nat. Rev. Microbiol.* **13**, 559–572 (2015).
2. Pierce, M. M., Raman, C. S. & Nall, B. T. Isothermal Titration Calorimetry of Protein–Protein Interactions. *Methods* **19**, 213–221 (1999).
3. Dam, T. K., Torres, M., Brewer, C. F. & Casadevall, A. Isothermal Titration Calorimetry Reveals Differential Binding Thermodynamics of Variable Region-identical Antibodies Differing in Constant Region for a Univalent Ligand. *J. Biol. Chem.* **283**, 31366–31370 (2008).

4. Wells, R. D. *et al.* DNA structure and gene regulation. *Prog. Nucleic Acid Res. Mol. Biol.* **24**, 167–267 (1980).
5. Buurma, N. J. & Haq, I. Advances in the analysis of isothermal titration calorimetry data for ligand–DNA interactions. *Methods* **42**, 162–172 (2007).
6. Salim, N. N. & Feig, A. L. Isothermal titration calorimetry of RNA. *Methods* **47**, 198–205 (2009).
7. Geschwindner, S., Ulander, J. & Johansson, P. Ligand Binding Thermodynamics in Drug Discovery: Still a Hot Tip? *J Med Chem* **58**, 6321–6335 (2015).
8. Renaud, J.-P. *et al.* Biophysics in drug discovery: impact, challenges and opportunities. *Nat Rev Drug Discov* **15**, 679–698 (2016).
9. Ladbury, J. E., Klebe, G. & Freire, E. Adding calorimetric data to decision making in lead discovery: a hot tip. *Nat. Rev. Drug Discov.* **9**, 23–27 (2010).
10. Ciulli, A. Biophysical screening for the discovery of small-molecule ligands. *Methods Mol. Biol. Clifton NJ* **1008**, 357–388 (2013).
11. Smirnovienė, J., Smirnovas, V. & Matulis, D. Picomolar inhibitors of carbonic anhydrase: Importance of inhibition and binding assays. *Anal Biochem* **522**, 61–72 (2017).
12. Myszka, D. G. & Rich, R. L. Implementing surface plasmon resonance biosensors in drug discovery. *Pharm Sci Technol Today* **3**, 310–317 (2000).
13. Patching, S. G. Surface plasmon resonance spectroscopy for characterisation of membrane protein–ligand interactions and its potential for drug discovery. *Biochim Biophys Acta Biomembr* **1838**, 43–55 (2014).
14. Olaru, A., Bala, C., Jaffrezic-Renault, N. & Aboul-Enein, H. Y. Surface Plasmon Resonance (SPR) Biosensors in Pharmaceutical Analysis. *Crit Rev Anal Chem* **45**, 97–105 (2015).
15. Krimmer, S. G. & Klebe, G. Thermodynamics of protein–ligand interactions as a reference for computational analysis: how to assess accuracy, reliability and relevance of experimental data. *J Comput Aided Mol Des* **29**, 867–883 (2015).

16. Callies, O. & Daranas, A. H. Application of isothermal titration calorimetry as a tool to study natural product interactions. *Nat Prod Rep* **33**, 881–904 (2016).

17. Falconer, R. J. Applications of isothermal titration calorimetry - the research and technical developments from 2011 to 2015: Review of Isothermal Titration Calorimetry from 2011 to 2015. *J Mol Recognit* **29**, 504–515 (2016).

18. Vega, S., Abian, O. & Velazquez-Campoy, A. On the link between conformational changes, ligand binding and heat capacity. *Biochim Biophys Acta Gen Sub* **1860**, 868–878 (2016).

19. Chaires, J. B. Calorimetry and Thermodynamics in Drug Design. *Annu Rev Biophys* **37**, 135–151 (2008).

20. Leavitt, S. & Freire, E. Direct Measurement of Protein Binding Energetics by Isothermal Titration Calorimetry. *Curr. Opin. Struct. Biol.* **11**, 560–566 (2001).

21. Pantoliano, M. W. *et al.* High-density miniaturized thermal shift assays as a general strategy for drug discovery. *J Biomol Screen* **6**, 429–440 (2001).

22. McDonnell, P. A. *et al.* Assessing compound binding to the Eg5 motor domain using a thermal shift assay. *Anal Biochem* **392**, 59–69 (2009).

23. Yanchunas, J. *et al.* Molecular basis for increased susceptibility of isolates with atazanavir resistance-conferring substitution I50L to other protease inhibitors. *Antimicrob Agents Chemother* **49**, 3825–3832 (2005).

24. Cimmperman, P. & Matulis, D. Protein Thermal Denaturation Measurements via a Fluorescent Dye. in *RSC Biomolecular Sciences* (eds. Podjarny, A., Dejaegere, A. P. & Kieffer, B.) vol. 0 247–274 (Royal Society of Chemistry, 2011).

25. Cimmperman, P. *et al.* A Quantitative Model of Thermal Stabilization and Destabilization of Proteins by Ligands. *Biophys J* **95**, 3222–3231 (2008).

26. Jarmoskaite, I., AlSadhan, I., Vaidyanathan, P. P. & Herschlag, D. How to measure and evaluate binding affinities. *eLife* **9**, (2020).

27. Schnapp, G., Klein, T., Hoevels, Y., Bakker, R. A. & Nar, H. Comparative Analysis of

Binding Kinetics and Thermodynamics of Dipeptidyl Peptidase-4 Inhibitors and Their Relationship to Structure. *J. Med. Chem.* **59**, 7466–7477 (2016).

28. *Biocalorimetry 2: applications of calorimetry in the biological sciences*. (Wiley, 2004).

29. Lafont, V. *et al.* Compensating Enthalpic and Entropic Changes Hinder Binding Affinity Optimization. *Chem. Biol. Drug Des.* **69**, 413–422 (2007).

30. Dullweber, F., Stubbs, M. T., Musil, Đ., Stürzebecher, J. & Klebe, G. Factorising ligand affinity: a combined thermodynamic and crystallographic study of trypsin and thrombin inhibition†. *J. Mol. Biol.* **313**, 593–614 (2001).

31. Rühmann, E., Betz, M., Heine, A. & Klebe, G. Fragment Binding Can Be Either More Enthalpy-Driven or Entropy-Driven: Crystal Structures and Residual Hydration Patterns Suggest Why. *J. Med. Chem.* **58**, 6960–6971 (2015).

32. Gaspari, R. *et al.* Kinetic and Structural Insights into the Mechanism of Binding of Sulfonamides to Human Carbonic Anhydrase by Computational and Experimental Studies. *J. Med. Chem.* **59**, 4245–4256 (2016).

33. Pulido, N. O. *et al.* On the molecular basis of the high affinity binding of basic amino acids to LAOBP, a periplasmic binding protein from *Salmonella typhimurium*: ENERGETIC BASIS OF LAOBP'S LIGAND RECOGNITION. *J. Mol. Recognit.* **28**, 108–116 (2015).

34. Hörtner, S. R. *et al.* Potent Inhibitors of tRNA-Guanine Transglycosylase, an Enzyme Linked to the Pathogenicity of theShigella Bacterium: Charge-Assisted Hydrogen Bonding. *Angew. Chem. Int. Ed.* **46**, 8266–8269 (2007).

35. Rechlin, C. *et al.* Price for Opening the Transient Specificity Pocket in Human Aldose Reductase upon Ligand Binding: Structural, Thermodynamic, Kinetic, and Computational Analysis. *ACS Chem. Biol.* (2017) doi:10.1021/acschembio.7b00062.

36. Cheng, R. K. Y. *et al.* Structural insight into allosteric modulation of protease-activated receptor 2. *Nature* **545**, 112–115 (2017).

37. Huschmann, F. U. *et al.* Structures of endothiapepsin-fragment complexes from

crystallographic fragment screening using a novel, diverse and affordable 96-compound fragment library. *Acta Crystallogr. Sect. F Struct. Biol. Commun.* **72**, 346–355 (2016).

38. Guan, R., Tyler, P. C., Evans, G. B. & Schramm, V. L. Thermodynamic Analysis of Transition-State Features in Picomolar Inhibitors of Human 5′-Methylthioadenosine Phosphorylase. *Biochemistry* **52**, 8313–8322 (2013).

39. Ren, J. *et al.* Thermodynamic and Structural Characterization of Halogen Bonding in Protein–Ligand Interactions: A Case Study of PDE5 and Its Inhibitors. *J. Med. Chem.* **57**, 3588–3593 (2014).

40. Krishnamurthy, V. M. *et al.* Thermodynamic parameters for the association of fluorinated benzenesulfonamides with bovine carbonic anhydrase II. *Chem. Asian J.* **2**, 94–105 (2007).

41. Brautigam, C. A., Zhao, H., Vargas, C., Keller, S. & Schuck, P. Integration and global analysis of isothermal titration calorimetry data for studying macromolecular interactions. *Nat. Protoc.* **11**, 882–894 (2016).

42. Kemmer, G. & Keller, S. Nonlinear least-squares data fitting in Excel spreadsheets. *Nat. Protoc.* **5**, 267–281 (2010).

43. Krainer, G. & Keller, S. Single-experiment displacement assay for quantifying high-affinity binding by isothermal titration calorimetry. *Methods* **76**, 116–123 (2015).

44. Krainer, G., Broecker, J., Vargas, C., Fanghänel, J. & Keller, S. Quantifying High-Affinity Binding of Hydrophobic Ligands by Isothermal Titration Calorimetry. *Anal Chem* **84**, 10715–10722 (2012).

45. Broecker, J., Vargas, C. & Keller, S. Revisiting the optimal cvalue for isothermal titration calorimetry. *Anal. Biochem.* **418**, 307–309 (2011).

46. Johnson, M. L. Evaluation and propagation of confidence intervals in nonlinear, asymmetrical variance spaces. Analysis of ligand-binding data. *Biophys. J.* **44**, 101–106 (1983).

47. Tellinghuisen, J. Statistical error in isothermal titration calorimetry: Variance function estimation from generalized least squares. *Anal. Biochem.* **343**, 106–115 (2005).

48. Tellinghuisen, J. Critique of methods for estimating heats in isothermal titration calorimetry. *Anal. Biochem.* **563**, 79–86 (2018).

49. Tellinghuisen, J. Can you trust the parametric standard errors in nonlinear least squares? Yes, with provisos. *Biochim. Biophys. Acta BBA - Gen. Subj.* (2017) doi:10.1016/j.bbagen.2017.12.016.

50. Tellinghuisen, J. A study of statistical error in isothermal titration calorimetry. *Anal. Biochem.* **321**, 79–88 (2003).

51. Wiseman, T., Williston, S., Brandts, J. F. & Lin, L. N. Rapid measurement of binding constants and heats of binding using a new titration calorimeter. *Anal Biochem* **179**, 131–137 (1989).

52. Scheuermann, T. H. & Brautigam, C. A. High-precision, automated integration of multiple isothermal titration calorimetric thermograms: new features of NITPIC. *Methods San Diego Calif* **76**, 87–98 (2015).

53. Motulsky, H. & Christopoulos, A. *Fitting Models to Biological Data Using Linear and Nonlinear Regression: A Practical Guide to Curve Fitting*. (Oxford University Press, 2004).

54. Bates, D. M. & Watts, D. G. *Nonlinear Regression Analysis and Its Applications*. (Wiley, 2007).